Progress In Electromagnetics Research C, Vol. 42, 83–94, 2013

A SIMPLE UWB ANTENNA WITH DUAL STOP-BAND PERFORMANCE USING RECTANGULAR SLOT AND STRIP LINE ENDED UP SHORTING PIN

Mohammad Akbari[1, *], Meghdad Khodaee[2], Saman Zarbakhsh[1], and Reza Gholami[3]

[1]Young Researchers and Elite Club, Central Tehran Branch, Islamic Azad University, Tehran, Iran

[2]Department of Electrical Engineering, Faculty of Engineering, Shahid Beheshti University, Tehran, Iran

[3]Shahid Sattari Aeronautical University of Science and Technology, Iran

Abstract—This paper presents a new rectangle-slot antenna for ultra wideband applications with 3.5/5.5 GHz dual stop-band characteristics. The antenna contains a simple square radiating patch and a rectangle-slot ground plane, which provides a wide bandwidth from 2.6 GHz up to 14.1 GHz. In order to obtain dual stop-band properties at 3.5 and 5.5 GHz, a rectangular-shaped slot is etched off the ground plane, and a strip line ended up a shorting pin is applied, respectively. The antenna is simple in configuration and has a compact dimension of $20 \times 22\,\text{mm}^2$. The proposed antenna is designed, simulated and fabricated. The measured results exhibit a acceptable agreement with the simulated data. The antenna provides nearly omnidirectional radiation patterns, relatively flat gain over the entire UWB frequency excluding the two stop bands.

1. INTRODUCTION

Nowadays, UWB communication system is appealing more and more attention because of its benefits such as low power consumption, high data rate transmissions as in the multimedia communications, robustness against jamming, and high degree of reliability. In UWB communication systems, one of the main subjects is the design of a

Received 2 June 2013, Accepted 6 July 2013, Scheduled 18 July 2013

* Corresponding author: Mohammad Akbari (akbari.telecom@gmail.com).

compact antenna whilst providing wideband characteristics over the whole operating band. Recently, intensive research works on UWB antenna design have been reported. There are a set of techniques to increase the impedance bandwidth in various papers including [1–3]. Problem of using the UWB in public applications is that the frequency range of 3.1 GHz to 10.6 GHz for UWB systems will cause interference to the existing wireless communication systems, such as the IEEE 802.16 standard for WiMAX system at 3.5 GHz (3.3–3.69 GHz) and the IEEE 802.11a standard for WLAN system at 5.5 GHz (5.15–5.825 GHz). In order to avoid such interferences along these bands, a UWB antenna with multiple stop-band characteristics is required. Different techniques have been proposed and developed in the literature to notch-out a single- or multi-frequency band(s) [4–9]. The most common technique for a band-stopping is inserting slots. Diverse slots have been proposed by many researchers to be inserted in the radiating element, ground plane, feeding line and vicinity of the radiating element [4, 5]. The fractal structure is used to obtain both size reduction and frequency band notched characteristic in UWB antennas [6, 7]. Because these structures are electronically small resonators with very high Qs, they can be considered as filters providing sharp notches or pass of certain frequency bands. Also electromagnetic band gap (EBG) structures are used to improve UWB antenna performance such as increasing the antenna's gain as well as produce a frequency stop-band characteristic [8, 9]. These aforementioned methods can obtain a good single or dual stop-band property, but some of them are with large size or complicated design procedure which makes them unsuitable for the UWB antennas themselves. In this letter, a new dual stop-band antenna with compact size of $22 \times 20\,\text{mm}^2$ is proposed. To achieve two stop bands, a new slot is etched off the ground and a new strip line is used.

2. ANTENNA STRUCTURE AND DESIGN

Based on several parametric studies, the geometry of the proposed dual stopband UWB antenna is depicted in Figure 1. The antenna is printed on a FR4 substrate with a relative permittivity of 4.4, thickness $h = 1\,\text{mm}$, and size of $22 \times 20\,\text{mm}^2$ or about $0.21\lambda \times 0.23\lambda$ at 3.2 GHz (the first resonance frequency). The antenna is excited using a $50\,\Omega$ microstrip line, with width $W_f = 1.8\,\text{mm}$ and length $L_f = 4.5\,\text{mm}$. The basic antenna structure consists of a square radiating patch, a feed line, and a ground plane with a rectangle-slot into it. By inserting a strip line ended up a shorting pin on the back, stop band at 3.5 GHz can be obtained while by etching a rectangular slot off the ground

plane, another stop band at centre frequency 5.5 GHz is achieved. The optimized values of the antenna design parameters are illustrated in Table 1.

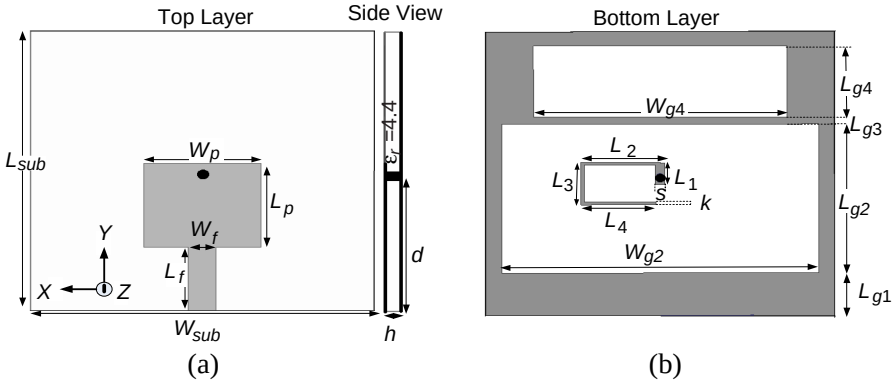

Figure 1. Geometry of the proposed dual stop-band UWB antenna. (a) Front and sideviews. (b) Back-view.

Table 1. Optimal dimensions of the antenna.

Prm.	(mm)	Prm.	(mm)	Prm.	(mm)	Prm.	(mm)
L_{sub}	20	W_{sub}	22	W_p	7.5	L_p	6
W_f	1.8	L_f	4.5	d	9.7	h	1
L_{g1}	3	L_{g2}	10.5	L_{g3}	0.5	L_{g4}	5
W_{g2}	20	W_{g4}	17	L_1	1.5	L_2	5.3
L_3	3	L_4	4.7	S	0.6	K	0.2

3. EFFECTS OF DIFFERENT PARAMETERS ON ANTENNA PERFORMANCE AND TIME-DOMAIN ANALYSIS

In this Section, we study the effects of the various parameters on the antenna performance and analyze the antenna in time domain. The parameters of the proposed antenna are studied by changing one or two parameters at a time and fixing the others. The simulated results are obtained using the Ansoft simulation software high-frequency structure simulator (HFSSTM) [10] and the antenna analysis in time domain are obtained using CST software [11]. In UWB systems, the information is transmitted using short pulses. Therefore, it is important to study

the temporal behavior of the transmitted pulse. The communication system for UWB pulse transmission must limit distortion, spreading and disturbance as much as possible. Group delay is an important parameter in UWB communication, which represents the degree of distortion of pulse signal. The key in UWB antenna design is to obtain a good linearity of the phase of the radiated field because the antenna should be able to transmit the electrical pulse with minimal distortion. Usually, the group delay is used to evaluate the phase response of the transfer function because it is defined as the rate of change of the total phase shift with respect to angular frequency. Ideally, when the phase response is strictly linear, the group delay is constant.

$$\text{group delay} = \frac{-d\theta(w)}{dw} \tag{1}$$

As depicted from Figure 2, the group delay variation for the antenna is presented, and the variation is approximately constant and less than 0.3 ns over the frequency band of interest except both resonant frequencies, 3.2 GHz and 8.4 GHz, which ensure that pulse transmitted or received by the antenna will not distort seriously and will retain its shape. Hence, the antenna is useful for modern UWB communication systems. Besides, Figure 2 also shows return loss of the antenna indicating both resonant frequencies and wide impedance bandwidth. Figure 3 depicts VSWR characteristics for three different antennas including the basic structure, with a strip line ended up shorting pin on the back plane, and the proposed antenna which their VSWR characteristics are compared to each other in Figure 3. In order to generate single stop band at centre frequency 3.5 GHz, we use the strip line ended up shorting pin while by etching a rectangular slot off the ground plane, another stop band at centre frequency 5.5 GHz is achieved.

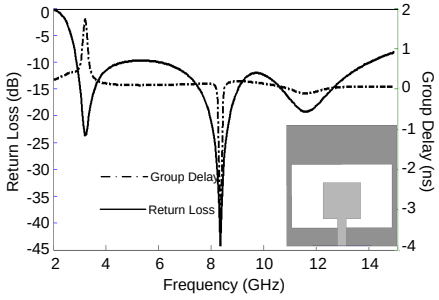

Figure 2. Group delay and return loss of the antenna.

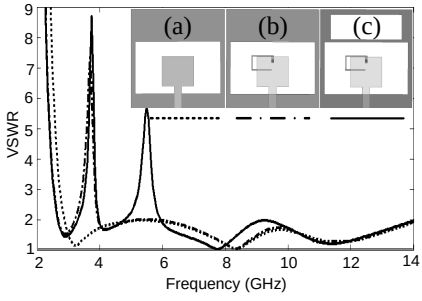

Figure 3. VSWR characteristics for various antennas.

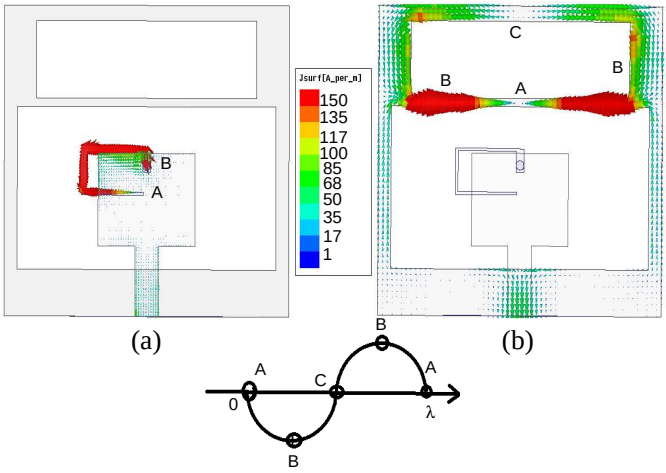

Figure 4. Simulated surface current distributions (a) on the strip line at 3.5 GHz and (b) around rectangular slot at top of the ground plane at 5.5 GHz.

To understand the phenomenon behind this dual stop-band performance, the simulated current distributions on the strip line and the ground plane at the stop frequencies of 3.5 GHz and 5.5 GHz are presented in Figures 4(a) and (b), respectively. It can be observed from Figure 4(a) that the current is concentrated on the edges of the interior and exterior of the strip line and the patch at frequency 3.5 GHz.

There is another point to note that the length of current circulation is nearly $\lambda/4$ because the current is increased from zero (point A) up to maximum (point B). From Figure 4(b) can be found that rectangular slot at top of the ground plane plays an important role on another notched band at centre frequency 5.5 GHz in a way that the most current is concentrated around it. The further point, the length of current circulation is nearly λ because the current is started from zero (point A), reaches to maximum with negative phase at (point B), then decrease to zero (point C), next it increases again to maximum with positive phase (point B), and at last goes back to the first place (at point A). Therefore, it is emphasized once again that the total length of current circulation is approximately λ. In this section, to exhibit being independent and controllable of both stop bands are applied Figures 5 to 7. As depicted in Figure 5, parameter L_4 has a markedly influence on frequency shifting for lower band stop. According to it, with increasing length L_4 the center frequency is decreased regularly in a way that by rising 1 mm in its length, centre frequency of the notched

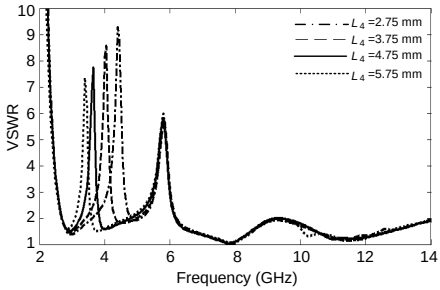

Figure 5. VSWR characteristics for the antenna with different values L_4.

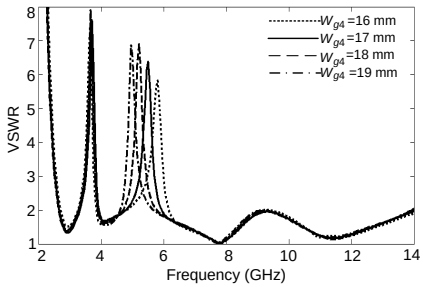

Figure 6. VSWR characteristics for the antenna with different values W_{g4}.

band is reduced about 0.5 GHz. The best value L_4 for covering 3.3 to 3.69 corresponds to 4.75 mm. As mentioned before, in this study to generate the stopband performance on Upper band with center frequency 5.5 GHz, is used an rectangular slot at top of the ground.

The simulated VSWR curves with different values W_{g4} are plotted in Figure 6. Related to it, when the length W_{g4} increases gradually, center frequency of the stop band is decreased steadily. Thus, the optimized W_{g4} is 17 mm. From these results, it can be found that the stop frequencies are controllable by changing the lengths L_4 and W_{g4}.

Parameter L_{g3}, meanwhile, plays a main role in increasing VSWR the upper stop band. As far as L_{g3} is concerned, the best of its value is 0.5 mm (Figure 7). Computation of the dispersion that occurs when the antenna radiates a pulse signal is also of interest.

The transmit transfer functions of the antennas were used to compute the radiated pulse in different directions when a reference signal was applied at the antenna input. This signal should present an UWB spectrum covering the antenna bandwidth and particularly the FCC mask from 3.1 to 10.6 GHz. It is shown in Figure 8 an acceptable approximation to a FCC mask compliant pulse can be obtained with a Gaussian seventh derivative. This pulse is represented in the time domain by:

$$G(t) = A \cdot \exp\left(\frac{-t^2}{2\delta^2}\right) \tag{2}$$

$$G^n(t) = \frac{d^n G}{dt^n} = (-1)^n \frac{1}{(\sqrt{2}\delta)^2} \cdot H_n\left(\frac{t}{\sqrt{2}\delta}\right) \cdot G(t) \tag{3}$$

$$H_7(t) = 128t^7 - 1344t^5 + 3360t^3 - 1680t \tag{4}$$

This signal and its spectrum are represented in Figure 8. The pulse

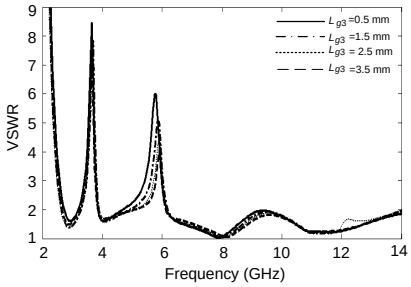

Figure 7. VSWR characteristics for the antenna with different values L_{g3}.

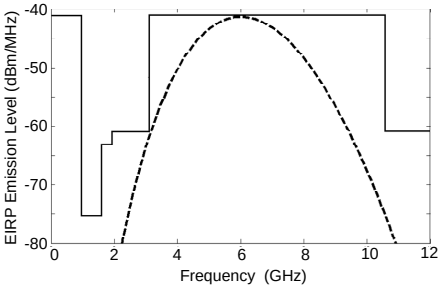

Figure 8. Power spectrum density compared to FCC mask.

bandwidth is exactly into mask desired. Unfortunately, this subject is paid less attention in many papers, and designers use Gaussian pulses with under seventh derivative that it can have tangible errors. Luckily, after drawing various Gaussian pulses from the first to eighth derivatives, it was obtained that the best pulse for covering FCC mask can be the seventh derivative.

Besides, with a bit tolerance, the sixth and eighth derivative are acceptable. A well-defined parameter named fidelity factor [12] is proposed to assess the quality of a received signal waveform regarding to the input signal, as given in Equation (5):

$$F = \max_{\tau} \left| \frac{\int_{-\infty}^{+\infty} S(t) r(t-\tau) dt}{\sqrt{\int_{-\infty}^{+\infty} S(t)^2 \cdot \int_{-\infty}^{+\infty} r(t)^2 dt}} \right| \tag{5}$$

where $S(t)$ and $r(t)$ are the TX and RX signals, respectively. For impulse radio in UWB communications, it is necessary to have a high degree of correlation between the TX and RX signals to avoid losing the modulated information. However, for most other telecommunication systems, the fidelity parameter is not that relevant. In order to evaluate the pulse transmission characteristics of the proposed antenna in the case of without notches, two configurations (side-by-side and face-to-face orientations) were chosen. The transmitting and receiving antennas were placed in a $d = 25\,\text{cm}$ distance from each other [13]. As shown in Figures 9 and 10, although the received pulses in each of two orientations are broadened, a relatively good similarity exists between the RX and TX pulses. By using (5), the fidelity factor for the side-by-side and face-to-face configurations was obtained which they equal 0.97 and nearly 0.94, respectively. These values for the fidelity factor

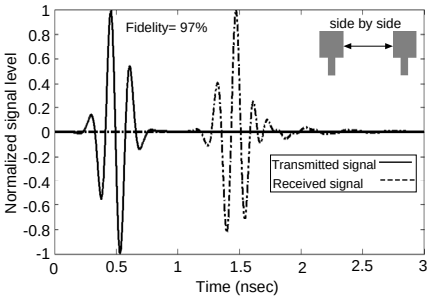

Figure 9. Transmitted and received pulses in time domain for a UWB link with identical antennas without notches in side-by-side orientation.

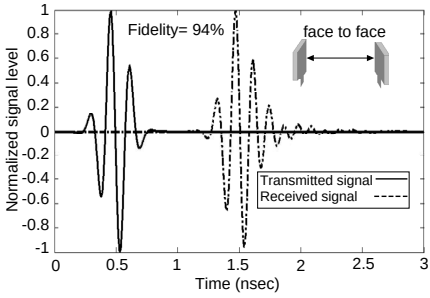

Figure 10. Transmitted and received pulses in time domain for a UWB link with identical antennas without notches in face-to-face orientation.

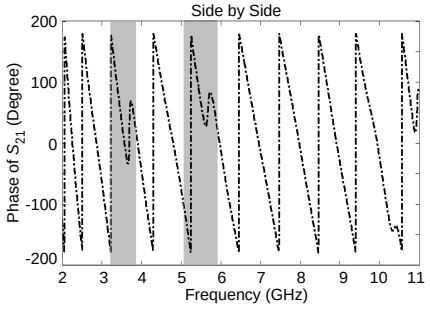

Figure 11. Simulated phase S_{21} with a pair of identical antennas.

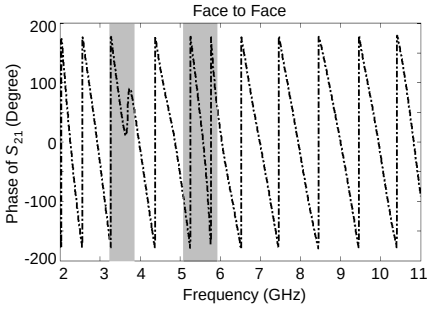

Figure 12. Simulated phase S_{21} with a pair of identical antennas.

show that the antenna imposes negligible effects on the transmitted pulses.

Phases S_{21} for side by side and face to face orientations are also illustrated in Figures 11 and 12. As previously expected, the plot shows a linear variation of phase in the total operating band except stop bands. It is important to note again that the distance between both the identical antennas in side by side and face to face orientations is 25 cm which has been extracted from [13].

The transmission coefficient S_{21} was simulated in the frequency domain for side by side and face-to-face orientations. Figures 13 and 14 exhibit the magnitude S_{21} for both cases of side by side and face to face. As it is apparent, magnitude S_{21} is almost flat with variation less than 10 dB in the operating band. The reason of two tangible

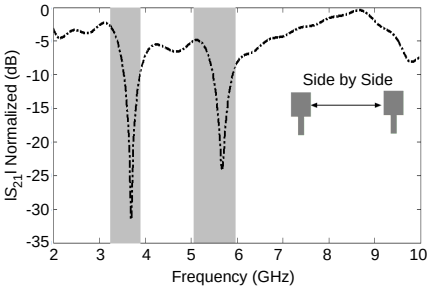

Figure 13. Simulated magnitude S_{21} with a pair of identical antennas.

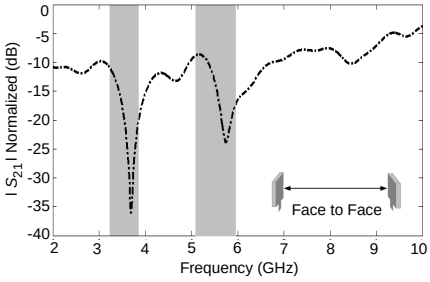

Figure 14. Simulated magnitude S_{21} with a pair of identical antennas.

resonances in magnitude S_{21} is due to two stop bands WiMAX and WLAN.

4. MEASUREMENT RESULTS AND DISCUSSIONS

The antenna was constructed and studied to demonstrate the effect of the proposed dual stopband function. The numerical and experimental results of the input impedance and radiation characteristics are presented and discussed.

The proposed antenna with optimal design was fabricated and tested in the Antenna Measurement Laboratory at Iran Telecommunication Research Center. The photo of the fabricated antenna is obvious in Figure 15.

Figure 15. Photograph of the fabricated antenna.

Figure 16 illustrates the measured and simulated VSWR characteristics of the proposed antenna. The fabricated antenna is able to cover the frequency band from 2.6 GHz to 14.1 GHz with two stop bands around 3.2 GHz to 3.8 GHz and 4.9 GHz to 6.1 GHz.

Figure 17 exhibits the measured gains of the antenna without

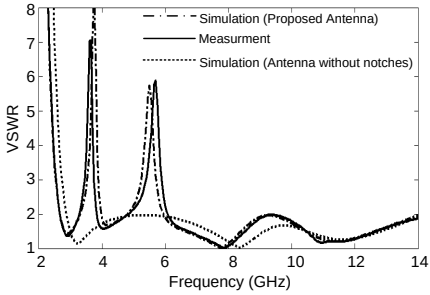

Figure 16. Measured and simulated VSWR for the proposed antenna.

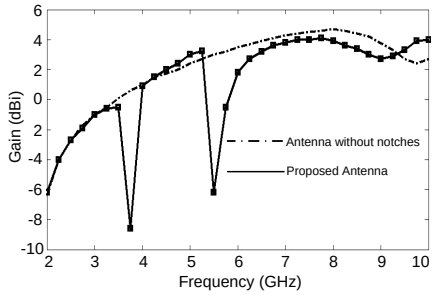

Figure 17. Measured gains of the proposed antenna without and with stop bands.

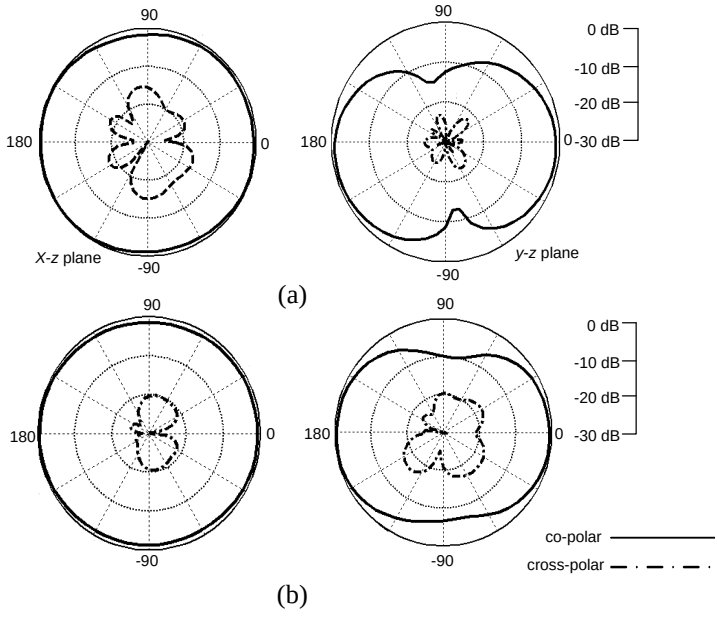

Figure 18. Measured radiation patterns of the antenna at (a) 4.5 and (b) 8 GHz.

and with stop bands. As shown in Figure 17, two sharp decrease of maximum gain on stop bands at 3.7 GHz and 5.5 GHz are obvious. For other frequencies outside stop bands, the antenna approximately has a flat gain. Figure 18 shows the measured normalized far-field radiation patterns in both H-plane (x-z plane) and E-plane (y-z plane) at frequencies 4.5 and 8 GHz. It can be observed that the radiation patterns in x-z plane are approximately omnidirectional for the two frequencies whereas radiation pattern in y-z plane are nearly bidirectional.

5. CONCLUSION

In this paper, a new compact UWB antenna with dual stop-band characteristics has been proposed. The fabricated antenna covers the impedance bandwidth of 2.6 GHz to 14.1 GHz with two stop bands around 3.2 GHz to 3.8 GHz and 4.9 GHz to 6.1 GHz. The proposed antenna has a simple configuration with a compact size $20 \times 22\,\text{mm}^2$ which is easy to fabricate. Experimental results indicate that the antenna can be a good candidate for UWB applications.

REFERENCES

1. Mighani, M., M. Akbari, and N. Felegari, "A novel SWB small rhombic microstrip antenna with parasitic rectangle into slot of the feed line," *Applied Computational Electromagnetics Society (ACES) Journal*, Vol. 27, No. 1, 74–79, January 2012.
2. Akbari, M., M. Koohestani, C. H. Ghobadi, and J. Nourinia, "A new compact planar UWB monopole antenna," *International Journal of RF and Microwave Computer-Aided Engineering*, Vol. 21, No. 2, 216–220, March 2011.
3. Akbari, M., M. Koohestani, C. Ghobadi, and J. Nourinia, "Compact CPW-fed printed monopole antenna with super wideband performance," *Microwave and Optical Technology Letters*, Vol. 53, No. 7, 1481–1483, July 2011.
4. Li, C. M. and L. H. Ye, "Improved dual band-notched UWB slot antenna with controllable notched bandwidths," *Progress In Electromagnetics Research*, Vol. 115, 477–493, 2011.
5. Mishra, S. K. and J. Mukherjee, "Compact printed dual band-notched U-shape UWB antenna," *Progress In Electromagnetics Research C*, Vol. 27, 169–181, 2012.
6. Ali, J. K., A. J. Salim, A. I. Hammoodi, and H. Alsaedi, "An ultra-wideband printed monopole antenna with a fractal based reduced

ground plane," *Progress In Electromagnetics Research Symposium Abstracts*, 330, Moscow, Russia, August 19–23, 2012.

7. Karmakar, A., S. Verma, M. Pal, and R. Ghatak, "An ultra wideband monopole antenna with multiple fractal slots with dual band rejection characteristics," *Progress In Electromagnetics Research C*, Vol. 31, 185–197, 2012.
8. Xu, F., Z. X. Wang, X. Chen, and X.-A. Wang, "Dual band-notched UWB antenna based on spiral electromagnetic-band gap structure," *Progress In Electromagnetics Research B*, Vol. 39, 393–409, 2012.
9. Saad, A. A. R., D. A. Salem, and E. E. M. Khaled, "5.5 GHz notched ultra-wideband printed monopole antenna characterized by electromagnetic band gap structures," *International Journal of Electronics and Communication Engineering (IJECE)*, Vol. 1, No. 1, 1–12, August 2012.
10. Ansoft High Frequency Structure Simulation (HFSSTM), Ver. 13, Ansoft Corporation, 2010.
11. CST Microwave Studio, Ver. 2008, Computer Simulation Technology, Framingham, MA, 2008.
12. Joardar, S. and A. B. Bhattacharya, "Two new ultrawideband dual polarized antenna-feeds using planar log periodic antenna and innovative frequency independent reflectors," *Journal of Electromagnetic Waves and Applications*, Vol. 20, No. 11, 1465–1479, 2006.
13. Medeiros, C. R., J. R. Costa, and C. A. Fernandes, "Compact tapered slot UWB antenna with WLAN band rejection," *IEEE Antennas and Wireless Propagation Letters*, Vol. 8, 661–664, 2009.